Supporting Information

A lanthanide based magnetic nanosensor as erasable and visible platform for multi-color point-of-care detection of multiple targets and the potential application by smartphone

Jun Xu[a], Xiao-KeShen[a], Lei Jia[a,*], Jian-Liang Cao[a], Yan Wang[b,*], Xiao-Lei Zhao[a], Ning Bi[a], Sheng-Li Guo[a], Tian-Yi Ma[c,*]

[a] *College of Chemistry and Chemical Engineering, Henan Polytechnic University, Jiaozuo 454000, China*

[b]*School of Safety Science and Engineering, State Key Laboratory Cultivation Base for Gas Geology and Gas Control, Henan Polytechnic University, Jiaozuo 454000, China*

[c]*Discipline of Chemistry, University of Newcastle, Callaghan, Newcastle, NSW 2308, Australia.*

*Corresponding authors. jlxj@hpu.edu.cn (L. Jia), yanwang@hpu.edu.cn (Y. Wang), tianyi.ma@newcastle.edu.au (T.Y. Ma)

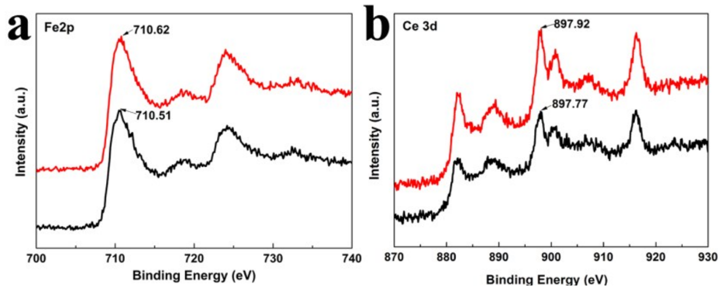

Fig. S1 XPS survey of Fe_3O_4@$CePO_4$:Tb (black) and Fe_3O_4@$CePO_4$:Tb-EDTA-Eu (red) samples: (a) Fe 2p and (b) Ce 3d.

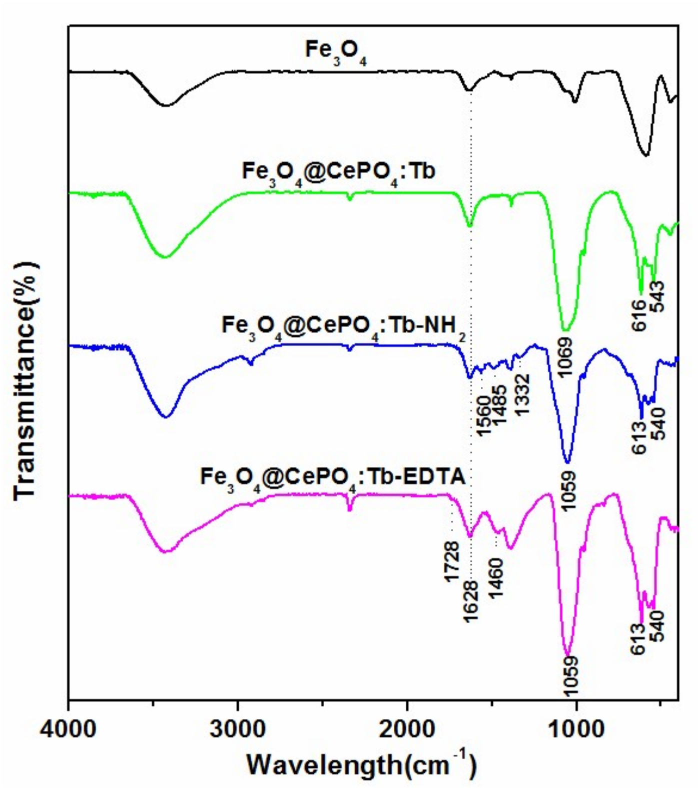

Fig. S2 The infrared spectra of Fe_3O_4, Fe_3O_4@$CePO_4$:Tb, Fe_3O_4@$CePO_4$:Tb-NH_2 and Fe_3O_4@$CePO_4$:Tb-EDTA.

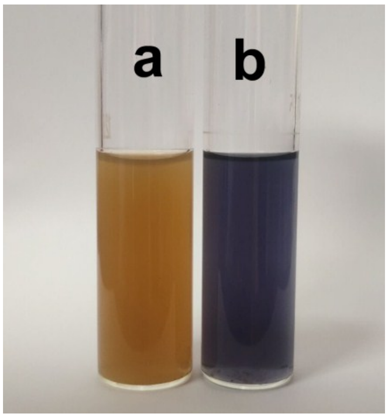

Fig. S3 The images of (a) Fe_3O_4@$CePO_4$:Tb-NH_2 nanocomposite in ethanol, (b) with the presence of Kaiser test reagents in a.

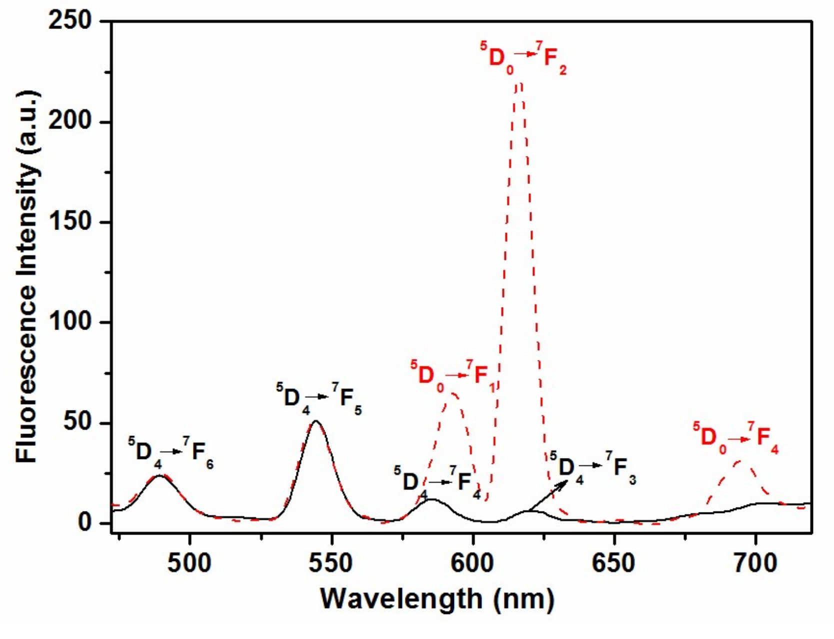

Fig. S4 Fluorescence spectra of Fe_3O_4@$CePO_4$:Tb-EDTA-Eu and that in the presence of 30μM DPA.

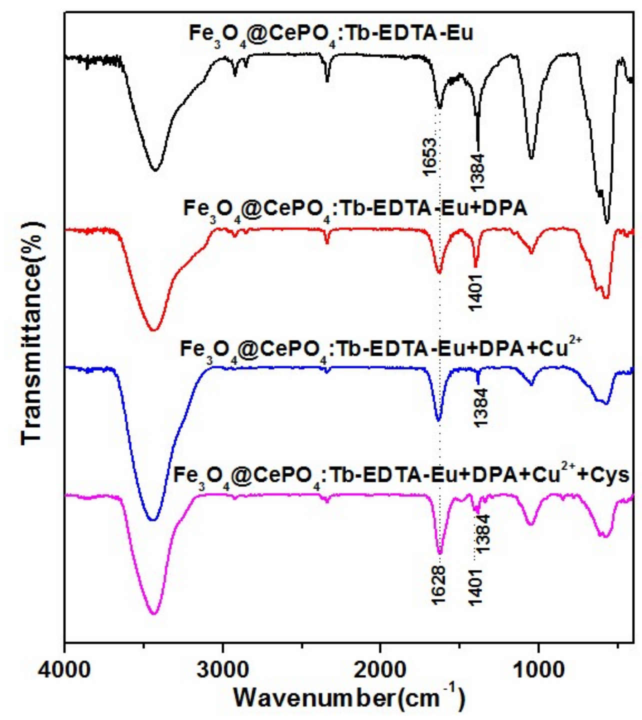

Fig. S5 The infrared spectra of Fe_3O_4@$CePO_4$:Tb-EDTA-Eu, Fe_3O_4@$CePO_4$:Tb-EDTA-Eu+DPA, Fe_3O_4@$CePO_4$:Tb-EDTA-Eu+DPA+Cu^{2+} and Fe_3O_4@$CePO_4$:Tb-EDTA-Eu+DPA+Cu^{2+}+Cys.

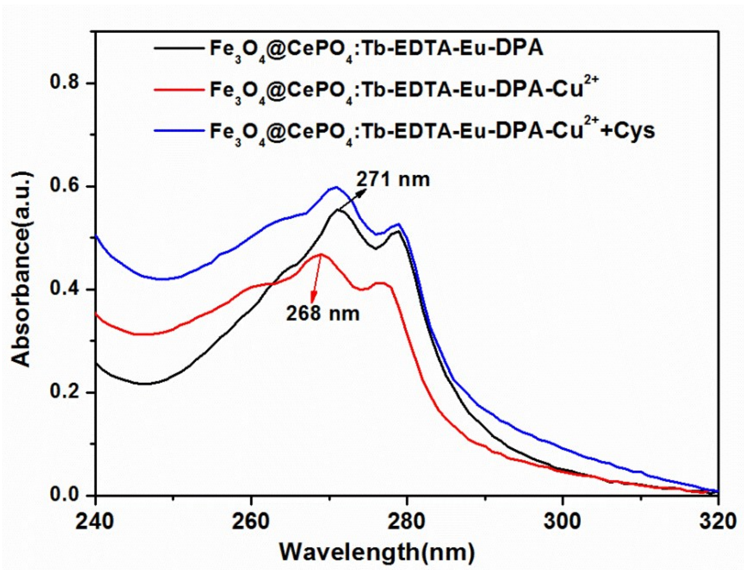

Fig. S6 UV-vis absorption spectrum of Fe_3O_4@$CePO_4$:Tb-EDTA-Eu-DPA (black), Fe_3O_4@$CePO_4$:Tb-EDTA-Eu-DPA-Cu (red), and Fe_3O_4@$CePO_4$:Tb-EDTA-Eu-DPA-Cu upon addition of Cys (blue).

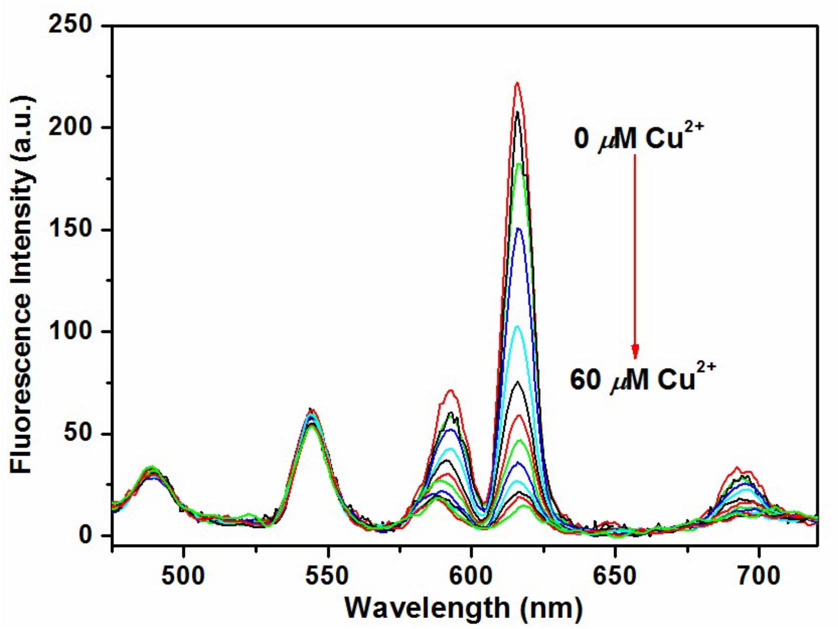

Fig. S7 Fluorescence spectra of Fe_3O_4@$CePO_4$:Tb-EDTA-Eu-DPA upon addition with increasing concentrations of Cu^{2+}.

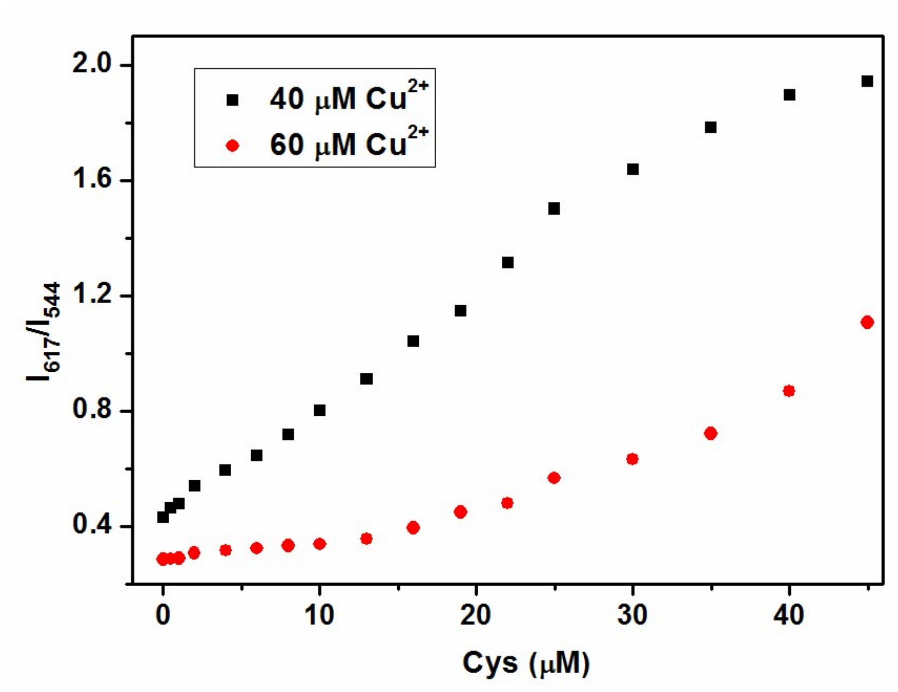

Fig. S8 The relative ratios of fluorescence intensity (I_{617}/I_{544})of Fe_3O_4@$CePO_4$:Tb-EDTA-Eu-DPA containing 40μM (black) or 60 μM (red) Cu^{2+} with increasing concentrations of Cys.

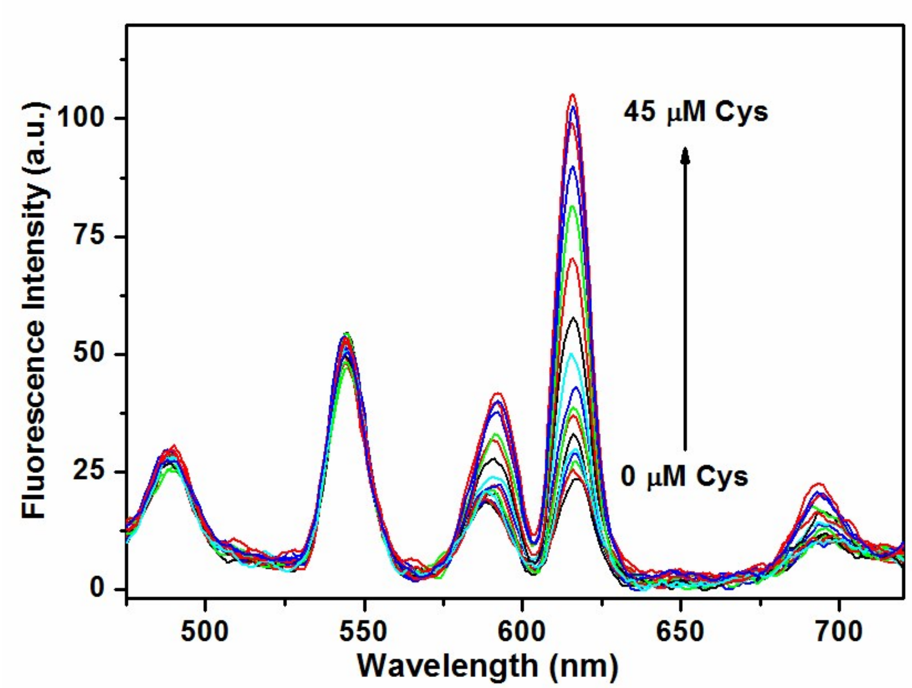

Fig. S9 Fluorescence spectra of Fe_3O_4@$CePO_4$:Tb-EDTA-Eu-DPA containing 40μM Cu^{2+} upon addition of different concentrations of cysteine from 0.0 to 45.0 μM.

Table S1 The color coordinates of CIE chromaticity diagram of Fe_3O_4@$CePO_4$:Tb-EDTA-Eunanoprobe for various concentrations of DPA (from 0 to 30.0 μM).

DPA concentrations(10^{-6}M)	0	0.05	0.1	0.5	1.0	1.5
x	0.258	0.256	0.256	0.263	0.268	0.289
y	0.377	0.377	0.362	0.367	0.356	0.358
DPA concentrations(10^{-6}M)	2.0	3.0	4.0	6.0	8.0	11.0
x	0.299	0.321	0.342	0.356	0.375	0.408
y	0.354	0.353	0.357	0.347	0.348	0.352
DPA concentrations(10^{-6}M)	14.0	18.0	22.0	26.0	30.0	
x	0.418	0.447	0.460	0.473	0.485	
y	0.350	0.352	0.350	0.351	0.344	

Table S2 Comparison of different methods for the determination of Cys.

Methods	Systems	Linear range (10^{-6}M)	Detection limit(10^{-6}M)	References
HPLC	N-ethylmaleimide	100–2000	50	1
fluorescence	QDs-Hg^{2+}	2.0–20	0.6	2
fluorescence	CdTe/CdSe quantum dots	0.2–100	0.131	3
fluorescence	Schiff-base-Cu^{2+}	50–200	0.05	4
fluorescence	Multi-color fluorescent probe	0.5–25	0.09	This work

Table S3 Analysis of Cys in urine samples (n = 3)

Spiked (10^{-6}M)	Found (10^{-6}M)	Recovery (%)	RSD (n=3) (%)
1	0.98 ± 0.04	98.03	1.34
5	4.97± 0.06	99.41	2.16
10	9.82± 0.06	98.63	2.55
25	24.45± 0.16	97.80	2.63

References

1. D. Giustarini, I. Dalle-Donne, A. Milzani and R. Rossi, *Anal. Biochem.,*2011, **415**, 81−83.

2. B. Han, J. Yuan and E. Wang, *Anal.Chem.,* 2009**, 81**, 5569−5573.

3. Y. Zhang, Y. Li and X. P. Yan, *Anal. Chem.,* 2009**, 81**, 5001−5007.

4. S. Das, Y. Sarkar, S. Mukherjee, J. Bandyopadhyay, S. Samanta, P. P. Parui and A. Ray, *Sensor Actuat. B-chem.,* 2015, **209**, 545−554.